Cellular and Molecular Bioengineering, Vol. 12, No. 1, February 2019 (© 2018) pp. 33–40
https://doi.org/10.1007/s12195-018-00560-1

Mechanical Response of an Epithelial Island Subject to Uniaxial Stretch on a Hybrid Silicone Substrate

YASHAR BASHIRZADEH, SANDEEP DUMBALI, SHIZHI QIAN, and VENKAT MARUTHAMUTHU

Mechanical & Aerospace Engineering, Old Dominion University, 4635 Hampton Blvd, 238e Kaufman, Norfolk, VA 23529, USA

(*Received 23 July 2018; accepted 10 October 2018; published online 19 October 2018*)

Associate Editor Pinar Zorlutuna oversaw the review of this article.

Abstract

Introduction—The mechanical response of large multi-cellular collectives to external stretch has remained largely unexplored, despite its relevance to normal function and to external challenges faced by some tissues. Here, we introduced a simple hybrid silicone substrate to enable external stretch while providing a physiologically relevant physical micro-environment for cells.

Methods—We micropatterned epithelial islands on the substrate using a stencil to allow for a circular island shape without restraining island edges. We then used traction force microscopy to determine the strain energy and the intercellular sheet tension within the island as a function of time after stretch.

Results—While the strain energy stored in the substrate for unstretched cell islands stayed constant over time, a uniaxial 10% stretch resulted in an abrupt increase, followed by sustained increase in the strain energy of the islands over tens of minutes, indicating slower dynamics than for single cells reported previously. The sheet tension at the island mid-line perpendicular to the stretch direction also more than doubled compared to unstretched islands. Interestingly, the sheet tension at the island mid-line parallel to the stretch direction also reached similar levels over tens of minutes indicating the tendency of the island to homogenize its internal stress.

Conclusions—We found that the sheet tension within large epithelial islands depends on the midline direction relative to that of the stretch initially, but not at longer times. We suggest that the hybrid silicone substrate provides an accessible substrate for studying the mechanobiology of large epithelial cell islands.

Keywords—Mechanobiology, Strain, Traction force, Sheet tension, Micropatterning.

INTRODUCTION

External mechanical stimuli are known to regulate physiological processes controlling tissue development, maintenance and disease.[15,16,33] Mechanotransduction of signals due to substrate/ECM stretch *via* focal adhesions and ion channels regulates growth, migration, proliferation and differentiation in different cell types.[14,30–32,34] Particular cell responses to stretch depend on both stretch direction and frequency. For instance, adherent cells specifically reorient perpendicular to the stretch direction for uniaxial cyclic strain.[17] The response of cells to stretch also depends on the extent of cell–cell interactions, with rheological properties evolving over time for stretched monolayers.[13]

A primary aspect of the mechanical response of cells is the change in the traction force exerted by the cells on the substrate upon stretch. Traction force exertion in human airway smooth muscle cells was impaired right after stretch-unstretch maneuvers.[18] Traction forces exerted by uniaxially stretched human alveolar single epithelial cells was greater than the baseline but it significantly weakened to a level lower than the baseline upon release.[12] Human umbilical vein endothelial cells also displayed traction forces that increased by 5–20% upon uniaxial stretch.[29] Under equibiaxial sustained stretch, an acute cell stiffening and enhancement of traction force was observed in smooth muscle cells before their gradual reduction.[20] The traction force and endogenous sheet tension of epithelial islands (of 80 μm diameter) increased upon application of equibiaxial stretch and returned to near baseline levels over a time scale of < 10 min.[7] However, the mechanical response of larger epithelial clusters adherent to substrates have remained largely unexplored.

Prior experimental systems to apply stretch and simultaneously measure cell-exerted traction forces have involved either polydimethylsiloxane (PDMS)-

Address correspondence to Venkat Maruthamuthu, Mechanical & Aerospace Engineering, Old Dominion University, 4635 Hampton Blvd, 238e Kaufman, Norfolk, VA 23529, USA. Electronic mail: vmarutha@odu.edu

based discontinuous silicone pillar/micro-structured substrates[8,20] or continuous substrates that consist of soft substrates like PAA gel coupled to hard PDMS using chemical treatment.[22] For stretch maneuvers implemented with hydrogels such as polyacrylamide (PAA) gel or matrigel, matrix hydraulics can be a factor that needs to be considered.[7,18] Thus, it is desirable to use a continuous substrate that is not a hydrogel, and therefore does not involve additional hydraulic effects, in cell stretch maneuvers.

Here, we show that elastic soft silicone substrates bound to hard PDMS are suitable for simultaneous stretch and traction force microscopy. We pattern large epithelial cell islands hundreds of μm in diameter, apply 10% uniaxial stretch and track temporal changes in the traction forces exerted by these islands. We find that traction forces exerted by these islands quickly increase initially, but then continue to increase slowly over tens of minutes, compared to that for single cells/smaller islands reported previously. We also find that the cell sheet tension in the island also increase several-fold both in the stretch direction and in a direction perpendicular to it. The results highlight the ability of epithelial cell islands to both homogenize and bear stress within the island.

METHODS

Cell Culture

MDCK II cells (generously provided by Daniel Conway, Virginia Commonwealth University) were cultured in DMEM (Dulbecco's modified Eagle's medium, Corning, Corning, NY) supplemented with L-Glutamine, sodium pyruvate, 1% Penicillin/Streptomycin, and 10% Fetal Bovine Serum (FBS) (Corning) at 37 °C and under 5% CO_2.

Preparation of Hybrid silicone Substrates

In a 60 mm petri dish, 0.85 g CY52-276 A/B (Dow Corning, Midland, MI, USA) with an A:B ratio of 1:1 was cast on a cured piece of hard PDMS (Sylgard184 Silicone Elastomer kit, Dow Corning Corp., Freeland, MI, USA) with pre-polymer to curing agent weight ratio of 10:1 for the hard PDMS. After 10 min of degassing, the soft silicone was cured on a hot plate at 70 °C for 30 min. The cured soft silicone was exposed to deep UV light for 5 min and the top surface was seeded with carboxylate fluorescent beads (Spherotech, Lake Forest, IL, USA) of 0.44 μm diameter as follows (Fig. 1). The sample was inverted[7] on a suspension containing 19 mg EDC (1-Ethyl-3-(3-dimethylaminopropyl)-carbodiimide) (Thermo fisher scientific, Waltham, MA, USA), 11 mg sulfo-NHS (*N*-Hydroxysulfosuccinimide) (Thermo fisher scientific, Waltham, MA, USA), 30 μL of 1% w/v fluorescent beads, and 0.02 mg of collagen I from rat tail (Corning Inc., Corning, NY) in 1 mL DI water for 30 min.[3,4] By incubation of the sample with this mixture, both fluorescent beads and collagen I were conjugated to the top surface of the soft silicone. Then, a slab of 45×35 mm^2 PDMS/soft silicone was cut and washed with PBS before it was used for micropatterning.

Micropatterning of Large Epithelial Cell Islands

12 mm thick 316 stainless steel sheets with laser-drilled 380 μm diameter holes (California Lasers, Simi Valley, CA, USA) were used as biocompatible stencils to topographically confine the plated epithelial cells. Briefly, a few drops of DMEM were pipeted onto the soft silicone sample before the perforated sheet was placed on the substrate. This step is critical as it avoids air entrapment in the sheet holes. Media with cells was then plated on top of the perforated sheet so that the cells settled on the substrate beneath the holes. After overnight incubation at 37 °C, 5% CO_2, micropatterned islands with the same size as that of the sheet holes were obtained.

Substrate Stretch

A custom designed uniaxial stretcher was used to uniaxially stretch micropatterned epithelial monolayers. The stretcher was designed using Autodesk Inventor, made of 316 stainless and machined at the Batten College of Engineering Machine shop at Old Dominion University. A 5/32'' screw essentially controlled the level of separation between two 10 mm beams (on which the PDMS sample would be clamped), with a pin preventing rotation of the beams with respect to each other. The gap between two screws on each side of the stretcher (along *x*–*x* in Fig. 1a) was 40 mm. Similar to previously designed uniaxial stretchers,[6,26] media for the micropatterned cells was confined within a PDMS well placed on the substrate that was mounted on the stretcher. Here, CY52276 A/B (i.e., soft silicone) was used as a mechanically characterized silicone substrate[19,27] which can be coated with different proteins to enhance cell attachment.[1,10]

Image Acquisition

Phase and fluorescence images of the cell islands were acquired with a Leica DMi8 epifluorescence inverted microscope (Leica Microsystems, Buffalo Grove, IL, USA) equipped with a Clara cooled CCD camera (Andor Technology Ltd, Belfast, Ulster, UK),

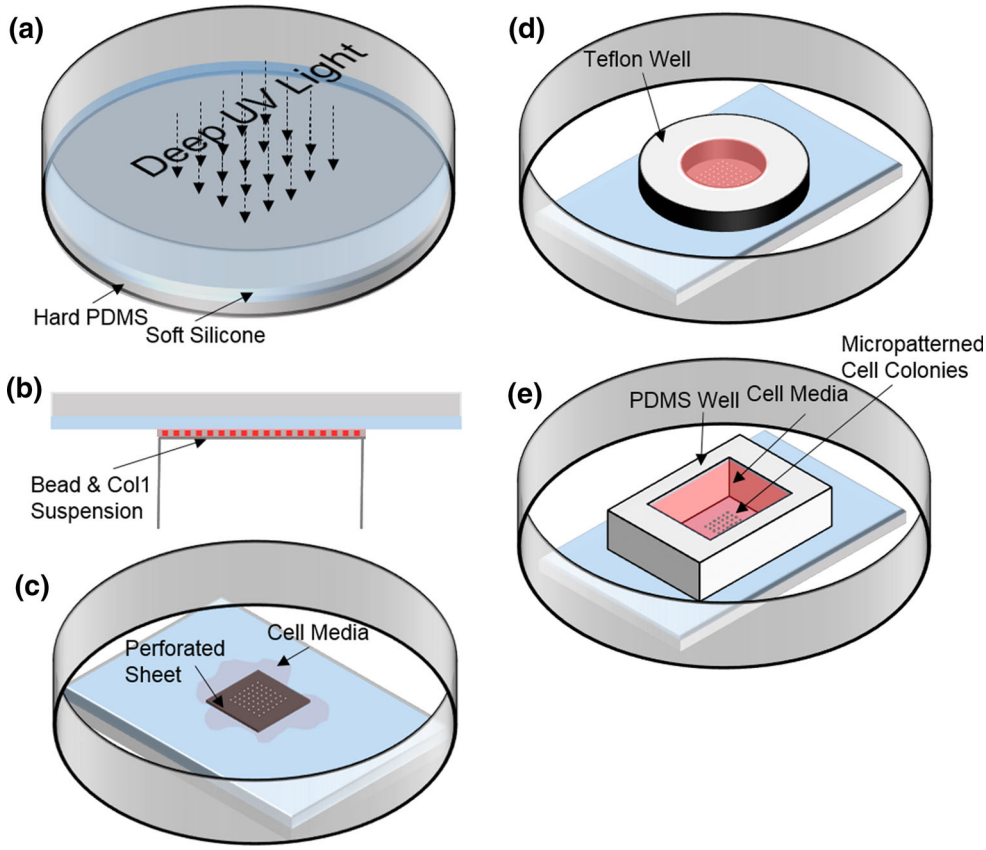

FIGURE 1. Preparation of hybrid silicone substrates and patterning of epithelial cell islands for stretch and traction measurements. Soft silicone was cured on a layer of pre-cured hard PDMS, and then exposed to deep UV light (of wave lengths 185 and 254 nm) (a). It was then incubated with an aqueous mixture containing EDC, sulfo-NHS, fluorescent beads, and collagen I in water (b). After washing with PBS, some cell culture media was added and a perforated stainless steel sheet was placed on the soft silicone sample (c). Cells were then plated in media constrained by a Teflon well (d). After overnight incubation at 37 °C (and 5% CO_2), the Teflon well and perforated sheet were removed and a PDMS well held replaced cell media supplemented with 10 mM HEPES (e).

a 10 × 0.3 NA objective lens, and an airstream incubator (Nevtek, Williamsville, VA, USA).

Immunofluorescence and E-cadherin/Actin Intensity Quantification

To perform immunofluorescence, the cells were fixed and permeabilized with 4% paraformaldehyde and 0.5% Triton-X. Primary antibody for E-cadherin (DECMA-1, Santa Cruz Biotechnology, Dallas, TX) and Alexafluor 488 conjugated phalloidin were used to stain E-cadherin and actin, respectively. Alexafluor 594 conjugated anti-rat secondary antibody was from Jackson ImmunoResearch, West Grove, PA. To quantify E-cadherin and actin intensity at the cell–cell contact, the intensity data for each frame was first normalized based on the exposure time. The average intensity of cell–cell contacts regions (of ~ 13 μm × 3.5 μm size each) pooled from the mid-region of the islands (for 105 contacts pooled from 21 unstretched islands and 132 contacts pooled from 44 stretched islands) were determined by using ImageJ. A 2-sample, 2-tail t-test assuming unequal variances was used for statistical analysis.

Substrate Strain Field

PIV was used to characterize the strain field of the substrate when stretched by 10% along the y direction. Captured substrate bead images before and after stretch were first preprocessed (e.g. adjustment of brightness/contrast) in ImageJ.[11,23] Then a direct cross-correlation PIV algorithm (PIVlab,[28] Version 1.42) in MATLAB (R2017a, MathWorks, Natick, MA, USA) with 256 × 256 pix^2 interrogation windows and 50% overlap yielded the displacement field (u, v) of the stretched substrate. After the application of post-processing (i.e., standard deviation filtering, local median filtering, data smoothing and removal of displacement at frame corners as outliers), the strain field of the substrate was computed as:

$$\varepsilon_{yy} = \frac{dv}{dy},\ \varepsilon_{xx} = \frac{du}{dx},\ \varepsilon_{xy} = \frac{1}{2}\left(\frac{du}{dy} + \frac{dv}{dx}\right) \quad (1)$$

Traction Force Microscopy

For control (unstretched) and stretched islands, red fluorescence bead images were taken over time as well as after the removal of the islands using 10% sodium dodecyl sulfate. PIVlab[28] (Version 1.42) was used to process image pairs (bead image of a time point and reference bead image). PIVlab was then used with the fast Fourier transform window deformation method with 50% overlapped interrogation windows of 64×64 and 32×32 pixel^2 to quantify the displacement of the beads resulting in a displacement vector field at each time point. The Young's modulus of the substrate (cured CY52-276 A/B) was previously measured to be 7.2 ± 2.4 kPa[3] using sphere indentation. By considering the substrate to be an elastic isotropic half space with Young's modulus of 7.2 kPa and Poisson's ratio of 0.5, Fourier transform traction cytometry[5,21,24,25] was used to compute the traction stress field using MATLAB.

Two-sample 2 tail student t-test was used to test the statistical significance of the effects of substrate stretch. Paired-sample 2 tail student t-test was used to test the statistical significance of temporal changes of associated variables. Significant effects are expressed as $*p < 0.05$, $**p < 0.01$, and $***p < 0.001$.

RESULTS

Compared to soft substrates such as PAA gels coupled to hard PDMS used previously[7,22] which require chemical treatments to bond the soft and hard substrates, we found that soft silicone bonded as it cured on hard PDMS without any need for chemical treatments. This substrate also avoids issues due to hydraulics observed previously with PAA bonded to PDMS.[7] We also devised a method to couple fluorescent micro-beads and collagen I just to the top surface of the soft silicone as depicted in Figs. 1a and 1b, drawing on previously published methods.[2] Using a custom built uniaxial stretcher (Fig. 2a), we assessed the strain field in the substrate as it was stretched by 10%. As shown in Fig. 2b, the strain along the stretch direction was 10%, with a strain magnitude about half that in the normal direction, as expected. The shear strain magnitude was more than an order of magnitude less.

We wanted to utilize this hybrid silicone substrate to assess how large epithelial cell islands mechanically responded to external stretch. We patterned large epithelial cell islands (Figs. 1c–1e) with a diameter of ~ 380 μm and with about six times as many cells as considered previously in 80 μm islands.[7] Figure 3a shows a map of traction stress exerted by an unstretched MDCK island. To characterize the mechanical output of the island, we quantified the strain energy stored in the substrate due to the work performed by the cell island,[5] computed as

$$W_A = \frac{1}{2}\int \vec{T}(r) \cdot \vec{u}(r) dA \quad (2)$$

where $\vec{u}(r)$ and $\vec{T}(r)$ are the displacement vector and the exerted traction stress vector applied by the cell island at a location of the substrate top surface, respectively. The strain energy density for an island is the strain energy divided by the cell island area.

Figure 3b shows the traction map for an MDCK island uniaxially stretched by 10%. Notice the apparent larger aspect ratio of the stretched island. As is evident in Fig. 3b, the overall levels of traction stress exerted are higher in stretched islands. Accordingly, compared to the unstretched islands, the stretched islands displayed higher strain energy density (Fig. 4). The strain energy density of stretched islands were significantly higher than unstretched islands even 5–10 min post-stretch ($p < 0.001$). However, the strain energy density after over an hour post-stretch was slightly even higher ($p < 0.05$) than at 5–10 min post-stretch, suggesting that the island mechanical response continues to evolve slowly.

In order to obtain a measure of forces transmitted through the cell island and from cell to cell, we then proceeded to quantify the sheet tension at the midline within the island[9] as follows: the net force exerted by the two halves of an island at the midline is given by

$$\vec{F}_i = \sum \overrightarrow{T_{ij}} \quad i = 1,\ 2 \quad (3)$$

where $\sum \overrightarrow{T_{ij}}$ is the vector sum of the traction forces over position j for each half i ($i = 1, 2$).

The average of these forces is the estimate for the net force at the island midline and the cell sheet tension per unit length is given by

$$\overrightarrow{F_L} = \frac{(\overrightarrow{F_1} - \overrightarrow{F_2})}{2L} \quad (4)$$

where L is the length of the island mid-line (i.e., the diameter of the island for unstretched islands). Compared to unstretched islands, the cell sheet tension for stretched cells at the midline (x–x) perpendicular to the stretch direction (y) was significantly higher ($p < 0.001$) even 5–10 min post-stretch (Fig. 5a). Interestingly, the cell sheet tension at the midline (y–y) parallel to the stretch direction (a) was also significantly higher ($p < 0.001$, Fig. 5b) compared to that

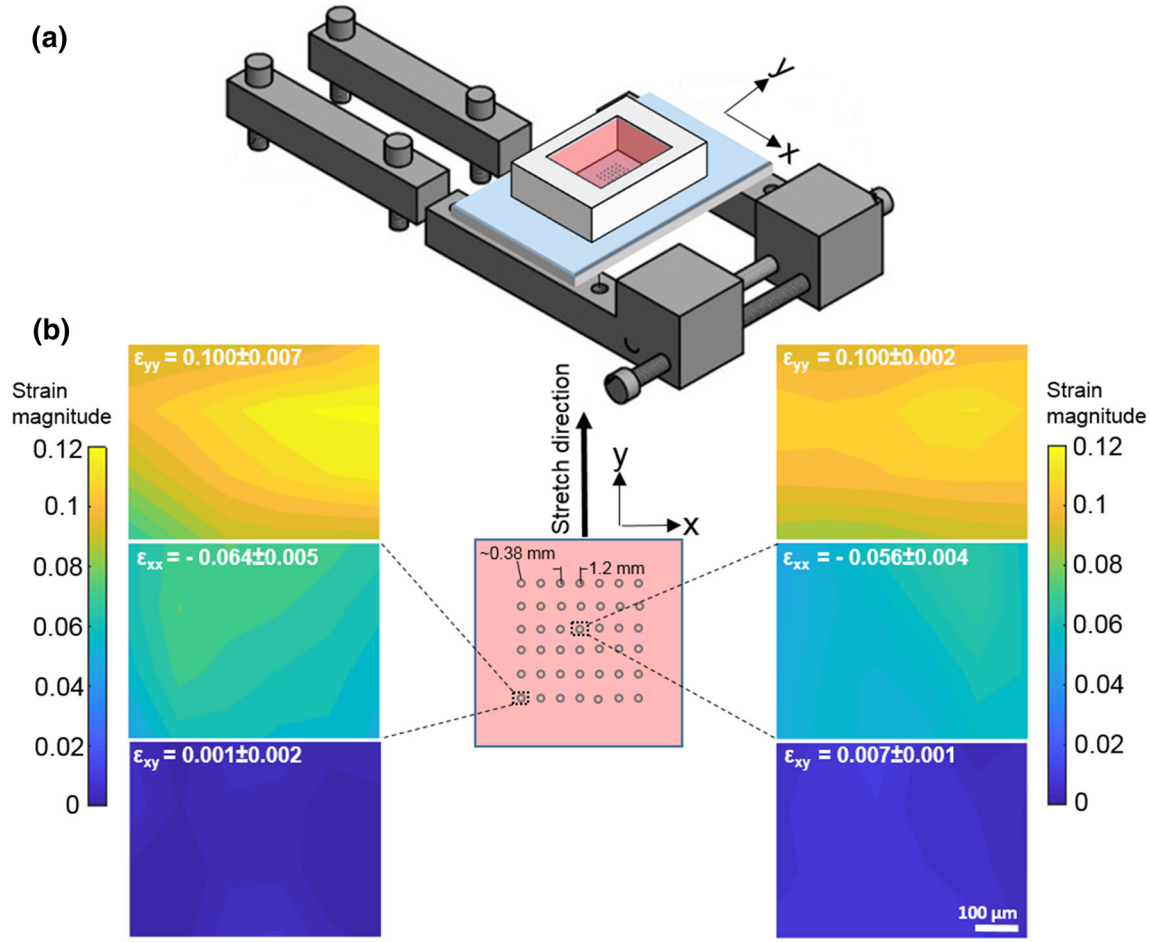

FIGURE 2. Application of uniaxial stretch. (a) Schematic of the custom designed uniaxial stretcher. (b) The region of the sample (where the islands are patterned, shown as circles) is schematically shown (middle), with y being the stretch direction. Strain field (ε_{yy}, ε_{xx}, ε_{xy}) of the substrate at the center (right images) and corner (left images) of the sample under 10% uniaxial stretch are shown.

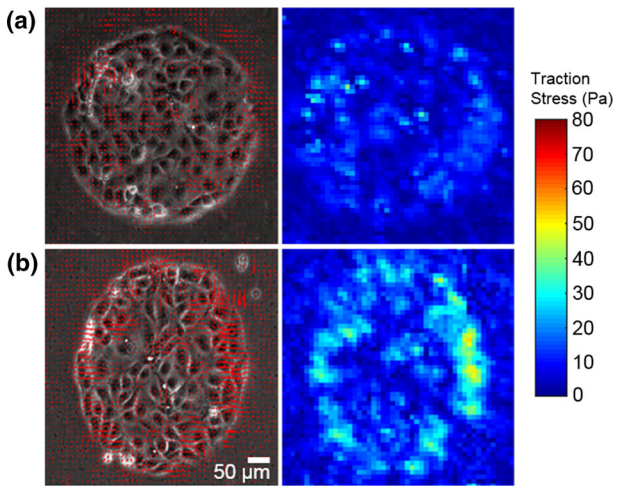

FIGURE 3. Traction forces exerted by control and uniaxially stretched MDCK islands. (a, b) Traction stress vector field (left) and traction stress magnitude (right) of a micropatterned MDCK cell island that hasn't been subjected to stretch (a) and that has been subjected to 10% uniaxial stretch (b) for 35–40 min.

for the unstretched islands 5-10 min post-stretch. While the cell sheet tension for stretched cells at the midline perpendicular to the stretch direction didn't change over tens of minutes, sheet tension at the midline parallel to the stretch direction was even higher over an hour post-stretch compared to just 5–10 min post-stretch ($p < 0.001$), indicating a slow increase. To assess if E-cadherin or actin level changes accompanied this increase in cell sheet tension, we used immunofluorescence to stain for E-cadherin and actin in unstretched and stretched islands (30 min post stretch, Fig. S1). Actin levels at the cell–cell contacts did not significantly differ between the unstretched and stretched islands (49.3 ± 29.5 arbitrary units (a.u) for unstretched case *vs.* 54.5 ± 28.8 a.u for stretched case, $p = 0.17$). E-cadherin levels at cell–cell contacts for stretched islands was marginally less than for unstretched islands (5.36 ± 2.43 arbitrary units (a.u) for unstretched case *vs.* 4.58 ± 2.57 a.u for stretched case, $p = 0.02$ for the null hypothesis).

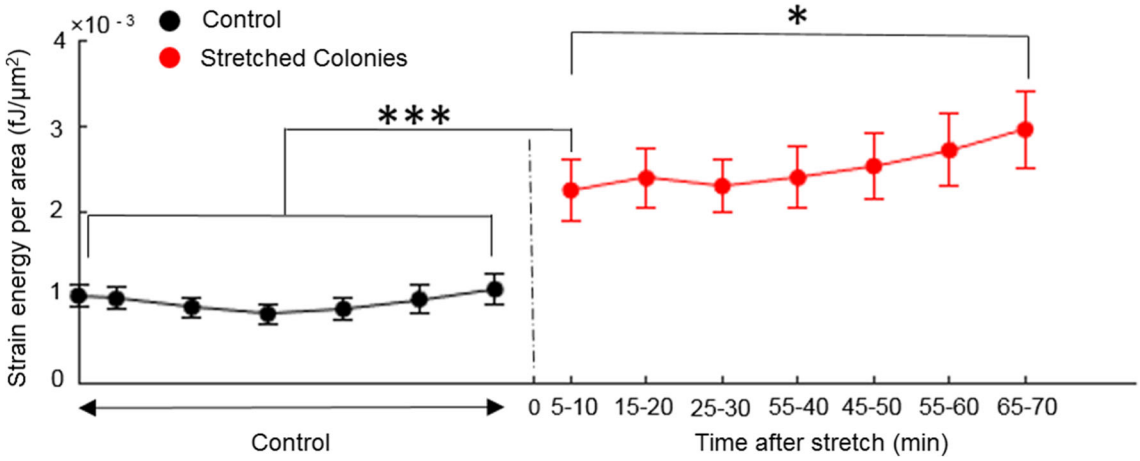

FIGURE 4. Temporal changes in strain energy density stored in the substrate for control (black) and stretched (red) cell islands. Strain energy per unit area of the control cell islands (*N* = 14 islands) stays essentially constant. Stretched islands (*N* = 17 islands) exhibit greater strain energy which continues to slowly increase over time after the initial abrupt increase. Error bars show the corresponding values of the standard error of the mean for all islands.

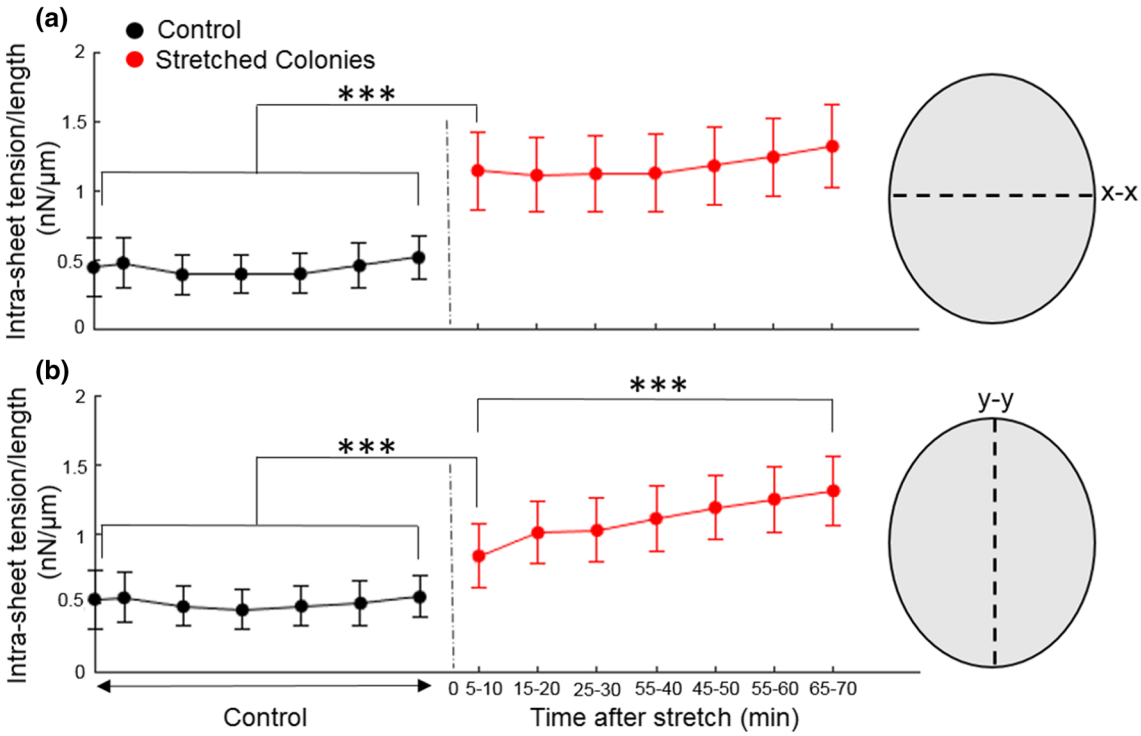

FIGURE 5. The sheet tension at the midline of control (black) (*N* = 14 islands) and stretched (red) (*N* = 17 islands) cell islands. Cell sheet tension of cell islands along the *x–x* (a) and *y–y* (b) midlines are shown. Error bars show the corresponding values of the standard error of the mean for all islands.

DISCUSSION AND CONCLUSION

We introduced a hybrid silicone substrate that can be fabricated relatively easily and avoids some of the steps (like chemical treatment for bonding) and complications (like hydraulic effects) of hydrogel-PDMS hybrid substrates.[7,22] Using stencil-based micro-patterning, we patterned large epithelial cell islands and uncovered aspects of their mechanical response to external stretch. We found that the density of strain energy stored in the substrate for stretched islands even at 5–10 min post-stretch was higher than that for unstretched islands. However, there was also a slow evolution of the strain energy density over tens of minutes, in contrast to that for single cells[20] and small islands[7] that exhibited smaller time scales for alter-

ations in exerted traction. Our data shows that this slower evolution is related to the slower increase in the cell sheet tension acting at the midline (y–y) parallel to the stretch direction (y), as it co-evolved with the strain energy density over tens of minutes. In contrast, the cell sheet tension acting at the midline (x–x) perpendicular to the stretch direction (y) maintained its magnitude over tens of minutes after the initial increase.

Our data indicate that epithelial islands under uniaxial stretch tend to homogenize their cell sheet tension in orthogonal directions over time, and that the time constants for these tension changes depend on the direction. The data also indicate that the cell sheet can sustain much higher increases in sheet tension (compared to baseline levels) without rupturing cell–cell contacts. This may reflect the inherent strength of the cell–cell contacts or rapid changes that help adapt the contacts to external challenges. Immunostaining of the islands did not show any significant increase in the extent of actin or E-cadherin localization at stretched cell–cell contacts (see "Methods") when compared to unstretched contacts (Fig. S1). However, we cannot strictly rule out subtle localized changes as there was large heterogeneity in the levels both E-cadherin and actin at the cell–cell contacts between islands. Future studies over longer time periods can reveal further changes that may occur in response to external stretch.

In vitro methods to exert external stretch on large cell collectives are essential to understand how multicellular collectives dynamically adapt and modify their behavior in response to external mechanical challenges. Understanding the response to a step increase in stretch can in turn help decipher responses to more complex stretch maneuvers. We propose that the hybrid substrates used here may enable enhanced studies of cell response to stretch as it facilitates both optical observations and force measurements.

ELECTRONIC SUPPLEMENTARY MATERIAL

The online version of this article (https://doi.org/10.1007/s12195-018-00560-1) contains supplementary material, which is available to authorized users.

ACKNOWLEDGMENTS

We thank Benedikt Sabass and Ulrich Schwarz for the script to reconstruct traction stresses. V.M. acknowledges support from the Thomas F. and Kate Miller Jeffress Memorial Trust and the National Institutes of Health under Award number 1R15GM116082.

FUNDING

This study was funded by NIH Grant 1R15GM116082.

CONFLICT OF INTEREST

Yashar Bashirzadeh, Sandeep Dumbali, Shizhi Qian and Venkat Maruthamuthu declare that they have no conflicts of interest.

ETHICAL APPROVAL

This article does not contain any studies with human participants or animals performed by any of the authors.

REFERENCES

[1]Anderson, D. E., and M. T. Hinds. Endothelial cell micropatterning: methods, effects, and applications. *Ann. Biomed. Eng*. 39:2329, 2011.
[2]Azioune, A., N. Carpi, Q. Tseng, M. Thery, and M. Piel. Protein micropatterns: a direct printing protocol using deep UVs. *Methods Cell Biol*. 97:133–146, 2010.
[3]Bashirzadeh, Y., S. Chatterji, D. Palmer, S. Dumbali, S. Qian, and V. Maruthamuthu. Stiffness measurement of soft silicone substrates for mechanobiology studies using a widefield fluorescence microscope. *J Vis Exp* 137:57797, 2018.
[4]Bashirzadeh, Y., S. Qian, and V. Maruthamuthu. Non-intrusive measurement of wall shear stress in flow channels. *Sens. Actuators A* 271:118–123, 2018.
[5]Butler, J. P., I. M. Tolic-Nørrelykke, B. Fabry, and J. J. Fredberg. Traction fields, moments, and strain energy that cells exert on their surroundings. *Am. J. Physiol*. 282:C595–C605, 2002.
[6]Carpi, N., and M. Piel. Stretching micropatterned cells on a PDMS membrane. *J. Vis. Exp*. 83:51193, 2014.
[7]Casares, L., R. Vincent, D. Zalvidea, N. Campillo, D. Navajas, M. Arroyo, and X. Trepat. Hydraulic fracture during epithelial stretching. *Nat. Mater*. 14:343, 2015.
[8]Cesa, C. M., N. Kirchgessner, D. Mayer, U. S. Schwarz, B. Hoffmann, and R. Merkel. Micropatterned silicone elastomer substrates for high resolution analysis of cellular force patterns. *Rev. Sci. Instrum*. 78:034301, 2007.
[9]Dumbali, S. P., L. Mei, S. Qian, and V. Maruthamuthu. Endogenous sheet-averaged tension within a large epithelial cell colony. *J. Biomech. Eng*. 139:101008, 2017.
[10]Feinberg, A. W., W. R. Wilkerson, C. A. Seegert, A. L. Gibson, L. Hoipkemeier-Wilson, and A. B. Brennan. Systematic variation of microtopography, surface chemistry and elastic modulus and the state dependent effect on

endothelial cell alignment. *J. Biomed. Mater. Res. Part A* 86:522–534, 2008.
[11]Ferreira, T., and W. Rasband. ImageJ user guide. ImageJ/Fiji 1. 2012.
[12]Gavara, N., P. Roca-Cusachs, R. Sunyer, R. Farré, and D. Navajas. Mapping cell-matrix stresses during stretch reveals inelastic reorganization of the cytoskeleton. *Biophys. J.* 95:464–471, 2008.
[13]Harris, A. R., L. Peter, J. Bellis, B. Baum, A. J. Kabla, and G. T. Charras. Characterizing the mechanics of cultured cell monolayers. *Proc. Natl. Acad. Sci. USA* 109:16449–16454, 2012.
[14]Hoffman, B. D., C. Grashoff, and M. A. Schwartz. Dynamic molecular processes mediate cellular mechanotransduction. *Nature* 475:316–323, 2011.
[15]Ingber, D. Mechanobiology and diseases of mechanotransduction. *Ann. Med.* 35:564–577, 2003.
[16]Janmey, P. A., and R. T. Miller. Mechanisms of mechanical signaling in development and disease. *J. Cell Sci.* 124:9–18, 2011.
[17]Jungbauer, S., H. Gao, J. P. Spatz, and R. Kemkemer. Two characteristic regimes in frequency-dependent dynamic reorientation of fibroblasts on cyclically stretched substrates. *Biophys. J.* 95:3470–3478, 2008.
[18]Krishnan, R., C. Y. Park, Y.-C. Lin, J. Mead, R. T. Jaspers, X. Trepat, G. Lenormand, D. Tambe, A. V. Smolensky, and A. H. Knoll. Reinforcement versus fluidization in cytoskeletal mechanoresponsiveness. *PLoS ONE* 4:e5486, 2009.
[19]Lee, E., M. L. Ewald, M. Sedarous, T. Kim, B. W. Weyers, R. H. Truong, and S. Yamada. Deletion of the cytoplasmic domain of N-cadherin reduces, but does not eliminate, traction force-transmission. *Biochem. Biophys. Res. Commun.* 478:1640–1646, 2016.
[20]Mann, J. M., R. H. Lam, S. Weng, Y. Sun, and J. Fu. A silicone-based stretchable micropost array membrane for monitoring live-cell subcellular cytoskeletal response. *Lab Chip* 12:731–740, 2012.
[21]Plotnikov, S. V., B. Sabass, U. S. Schwarz, and C. M. Waterman. High-resolution traction force microscopy. *Methods Cell Biol.* 123:367–394, 2014.
[22]Quinlan, A. M. T., L. N. Sierad, A. K. Capulli, L. E. Firstenberg, and K. L. Billiar. Combining dynamic stretch and tunable stiffness to probe cell mechanobiology in vitro. *PLoS ONE* 6:e23272, 2011.
[23]Rasband, W. S. Imagej, us national institutes of health, Bethesda, MA, USA. 2011. http://imagej.nih.gov/ij/.
[24]Sabass, B., M. L. Gardel, C. M. Waterman, and U. S. Schwarz. High resolution traction force microscopy based on experimental and computational advances. *Biophys. J.* 94:207–220, 2008.
[25]Schwarz, U. S., N. Q. Balaban, D. Riveline, A. Bershadsky, B. Geiger, and S. Safran. Calculation of forces at focal adhesions from elastic substrate data: the effect of localized force and the need for regularization. *Biophys. J.* 83:1380–1394, 2002.
[26]Shao, Y., X. Tan, R. Novitski, M. Muqaddam, P. List, L. Williamson, J. Fu, and A. P. Liu. Uniaxial cell stretching device for live-cell imaging of mechanosensitive cellular functions. *Rev. Sci. Instrum.* 84:114304, 2013.
[27]Style, R. W., R. Boltyanskiy, G. K. German, C. Hyland, C. W. MacMinn, A. F. Mertz, L. A. Wilen, Y. Xu, and E. R. Dufresne. Traction force microscopy in physics and biology. *Soft Matter* 10:4047–4055, 2014.
[28]Thielicke, W., and E. Stamhuis. PIVlab–towards user-friendly, affordable and accurate digital particle image velocimetry in MATLAB. *J. Open Res. Softw.* 2:e30, 2014.
[29]Tsukamoto, A., K. R. Ryan, Y. Mitsuoka, K. S. Furukawa, and T. Ushida. Cellular traction forces increase during consecutive mechanical stretching following traction force attenuation. *J. Biomech. Sci. Eng.* 12:17-00118, 2017.
[30]Vogel, V., and M. Sheetz. Local force and geometry sensing regulate cell functions. *Nat. Rev. Mol. Cell Biol.* 7:265–275, 2006.
[31]Waters, C. M., K. M. Ridge, G. Sunio, K. Venetsanou, and J. I. Sznajder. Mechanical stretching of alveolar epithelial cells increases Na + -K + -ATPase activity. *J. Appl. Physiol.* 87:715–721, 1999.
[32]Wirtz, H. R., and L. G. Dobbs. Calcium mobilization and exocytosis after one mechanical stretch of lung epithelial cells. *Science* 250:1266–1270, 1990.
[33]Wozniak, M. A., and C. S. Chen. Mechanotransduction in development: a growing role for contractility. *Nat. Rev. Mol. Cell Biol.* 10:34–43, 2009.
[34]Yano, S., M. Komine, M. Fujimoto, H. Okochi, and K. Tamaki. Mechanical stretching in vitro regulates signal transduction pathways and cellular proliferation in human epidermal keratinocytes. *J. Investig. Dermatol.* 122:783–790, 2004.